

# A Review of Wireless SAW Sensors

Alfred Pohl, *Member, IEEE*

(*Invited Paper*)

**Abstract**—Wireless measurement systems with passive surface acoustic wave (SAW) sensors offer new and exciting perspectives for remote monitoring and control of moving parts, even in harsh environments. This review paper gives a comprehensive survey of the present state of the measurement systems and should help a designer to find the parameters required to achieve a specified accuracy or uncertainty of measurement.

Delay lines and resonators have been used, and two principles have been employed: SAW one-port devices that are directly affected by the measurand and SAW two-port devices that are electrically loaded by a conventional sensor and, therefore, indirectly affected by the measurand. For radio frequency (RF) interrogation, time domain sampling (TDS) and frequency domain sampling (FDS) have been investigated theoretically and experimentally; the methods of measurement are described. For an evaluation of the effects caused by the radio interrogation, we discuss the errors caused by noise, interference, bandwidth, manufacturing, and hardware tuning. The system parameters, distance range, and measurement uncertainty are given numerically for actual applications. Combinations of SAW sensors and special signal processing techniques to enhance accuracy, dynamic range, read out distance, and measurement repetition rate (measurement bandwidth) are presented. In conclusion, an overview of SAW sensor applications is given.

## I. INTRODUCTION

SENSOR technology is rapidly growing. For a wide variety of sensor applications, a fixed wired connection between the sensor and the evaluation unit cannot be established. Usage of slip-rings and brushes, however, cause additional mechanical and electrical problems (i.e., interruptions, noise, etc.), making these methods unusable in reliable systems. For these, radio sensors must be implemented.

The radio sensors can be divided into active devices, powered by a battery; semi active devices, energized by inductive coupling or by a strong RF signal; and passive transponder devices.

A radio sensor system generally employs a radio request unit and one or more distant sensor units. The radio interrogation consists of the radio request and the sensor response and its evaluation. The radio request signal is transmitted from the transmitter section of the interrogation system to the sensor (downlink). The sensor responds with a radio signal (uplink) that is received by the receiver

section of the interrogation system. Up- and downlink, the request signal and the sensor's response, have to be separated. A separation in frequency (frequency domain division; FDD) requires a frequency conversion or at least a nonlinear device in the sensor unit. Detecting the harmonics, the set up can be used for ID purposes. Utilizing intermodulation of the requesting signals, analog sensor information can be gained wirelessly [1]. A separation in space is difficult for linear passive or semi active devices; a separation between request and response signal in time (time domain division; TDD) is necessary, requiring an energy storage mechanism.

This paper focuses on the radio request of passive SAW devices published a few years ago as radio sensors [2], [3]. These passive devices re-transmit a linearly distorted version of the radio request signal. The distortion is affected by the measurand. The energy of the RF radio signal is stored in the SAW, which yields the required time delay between request signal and sensor response for TDD.

Because effects of the sensor device on the RF radio request signal have to be evaluated, the signal processing effort in the radio request system is much higher for passive devices than for active and semi active sensor circuits, responding with a digital data telegram. The received response signal is afflicted with noise and interference. Errors occurring during transmission yield additional contributions to the total measurement uncertainty.

Radio sensors and the request systems are radio systems and are ruled by the national governmental regulations. For industrial, scientific, and medical (ISM) applications, frequency bands are allocated. Keeping the limits concerning bandwidth and the effective isotropically radiated power (EIRP), the rules for short range devices (SRD) and low power devices (LPD) with reduced licensing requirements can be applied. In Europe, the limits of operation of radio sensors can be found in the ETSI CEPT/ERC 70-03 regulations EN300330 (9 kHz to 25 MHz), EN300220 (25 MHz to 1 GHz), and EN300440 (1 to 25 GHz).

In Section II, the SAW sensors are discussed briefly. Then, in Section III, the basic methods of radio interrogation are presented; block diagrams of the employed systems are given. Methods of parameter detection for energy enhancement and for multiple access are discussed; measures for data reduction are shown. After considering the properties and the effects of the radio channel in Section IV, in Section V, the deterministic and stochastic errors disturbing the sensor response detection are investigated. An estimation of measurement performance versus the distance range and the permissible error are given in Section VI. In

Manuscript received June 21, 1999; accepted November 16, 1999.

The author is with University of Technology Vienna, E3592, Applied Electronics Laboratory, A-1040 Vienna, Austria (e-mail: alfred.pohl@tuwien.ac.at).

Section VII, exemplary applications of SAW radio sensors are shown.

## II. PASSIVE SAW SENSORS

The application spectrum of SAW devices includes sensors as well as reference devices, employing the sensitivity of special crystal cuts of different substrate materials to temperature, mechanical stress, and strain, etc., or their stability against such. For application, the SAW sensor device is directly affected by the measurand; the sensitivity of the device against this physical quantity is utilized.

One of the most important effects on reference and sensor devices is the temperature coefficient (TK). The first experimental applications of SAW radio sensors have been focused on temperature measurements.

The materials commonly employed for SAW devices and for sensors are quartz ( $\text{SiO}_2$ ) (TK of quartz substrates has a wide minimum for room temperature and is neglected in many applications: “quartz stable operation”), lithium-niobate ( $\text{LiNbO}_3$ ), and lithiumtantalate ( $\text{LiTaO}_3$ ). New high temperature materials are berlinite ( $\text{AlPO}_4$ ), lithium tetraborate ( $\text{Li}_2\text{B}_4\text{O}_7$ ), langasit ( $\text{La}_3\text{Ga}_5\text{SiO}_{14}$ ), and galliumorthophosphate ( $\text{GaPO}_4$ ), applicable up to  $1000^\circ\text{C}$ . Usually, the circuits and enclosures the SAW device is implemented into limit the operation range of the complete sensor to a much narrower range than the SAW device itself. In Table I, the linear TK at room temperature is given for common SAW substrate materials.

Apart from temperature, the propagation of the SAW depends on the geometry of the substrate and the material parameters subject to environmental conditions. In Table II, the achievable linear coefficients for physical effects to SAW substrates are summarized [4].

Effecting the substrate directly by the measurand yields sensor capability. For radio sensor application, a one-port reflective SAW device is connected to an antenna and requested by an RF radio signal [2], [3]. Initially, these circuits have been invented for the wireless identification (RF ID) of animals [11]. Until now, a wide range of prototype applications has been published [5]–[10].

The first industrial application is a road pricing system for the Norwegian highways around Oslo [12].

The RF operation frequency is limited by the substrate size and by the photolithographic process. SAW devices are manufactured in the frequency range between 30 MHz and approximately 3 GHz.

The currently applied types of SAW radio sensors are discussed now with a brief summary of applications in Section VII.

The radio interrogation system transmits an RF signal and then switches to receive mode. After a time delay, the convolution of the radio request signal and the reflective SAW device’s RF response (burst response, if a burst was transmitted), carrying the information of the measurand, is transmitted back to the receiver.

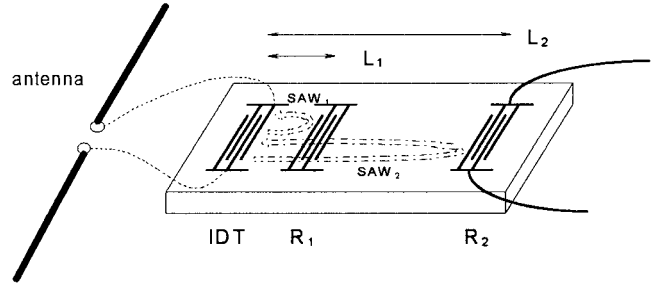


Fig. 1. One-port wideband SAW DL.

As directly affected SAW radio sensors, wideband and dispersive delay lines have been implemented as well as one-port SAW resonators. SAW delay lines utilize the SAW propagation time  $T_D = L/v_{\text{SAW}}$ , the ratio of acoustical length and SAW velocity. In known sensor applications,  $L$  and  $v_{\text{SAW}}$ , respectively, are changed because of a temperature change, mechanical stress, and strain and because of a mass loading from a thin surface layer.

The delay ( $T_0$ ) of a delay line (DL) is affected by the measurand  $y$ . With the relative sensitivity  $S_T^y = \frac{1}{T} \cdot \frac{dT}{dy}$  of the parameter  $T$  for the effect  $y$ , a linear approximation of the resulting delay yields

$$T_y = T_0 (1 + S_T^y \cdot y) = T_0(1 + \epsilon). \quad (1)$$

The sensor effect yields a scaling of the delay time by a factor  $1 + \epsilon$ . The variation  $\Delta T$  of a time delay  $T_0$  is  $\Delta T = T_y - T_0 = T_0 \cdot S_T^y \cdot y$ . Generally, to avoid errors caused by cross sensitivities for temperature, etc., differential measurements of delay or center frequency are performed.

In Fig. 1, a one-port wideband SAW DL is sketched. The device is interrogated by an RF signal. If the sensor’s bandwidth is assumed to be wider than that of the signal, the sensor’s response consists of delayed versions of the request signal.

For identification purposes, the reflectors are used as bits of a serial response data word with a pulse amplitude modulation (usually an on/off keying), a pulse position modulation, or a pulse phase modulation.

For measurements, the sensor effect causes a scaling of the sensor impulse response (a shift in delay  $(L_2 - L_1)/v_{\text{SAW}}$  between the reflectors at positions  $L_1$  and  $L_2$ ) or a modulation of the SAW attenuation and, therefore, a pulse amplitude modulation.

Dispersive SAW devices are well known for matched filter applications, e.g., for chirp impulse compression in RADAR systems [13]. A mismatch of the signal and the compressor, e.g., if Doppler shift occurs in radio transmission systems, yields a time shift of the compressed impulse and, therefore, an error in distance evaluation. On the other hand, it is useful applied in compressive receivers. As shown in [14], by employing impulse compression for sensor purposes, a gain in sensitivity is achieved in comparison with the wideband delay line sensor.

A recently invented new type of two-port SAW radio transponders avoids the direct effect to the substrate but

TABLE I  
LINEAR TK AT ROOM TEMPERATURE FOR SAW SUBSTRATE MATERIALS.

Substrate material	Crystal cut	Linear TK
Lithiumniobate LiNbO <sub>3</sub>	rotated 128 Y/X cut	72 ppm/K
	Y/Z standard cut	92 ppm/K
Lithiumtantalate LiTaO <sub>3</sub>	X/112Y	18 ppm/K
	36 Y/X rotated cut	30 ppm/K
Langasit (La <sub>3</sub> Ga <sub>5</sub> SiO <sub>14</sub> )	X/Y cut	24 ppm/K
Quartz (SiO <sub>2</sub> )	ST-X cut	0 ppm/K
		“Quartz stable”

TABLE II  
LINEAR COEFFICIENTS FOR PHYSICAL EFFECTS ON SAW SUBSTRATE MATERIALS.

Physical quantity	Linear coefficient
Temperature	up to 100 ppm/K
Pressure, stress	2 ppm/kPa
Force	10 ppm/kN
Mass loading	30 ppm/ $\mu\text{g}\cdot\text{cm}^2$
Voltage	1 ppm/V
Electric field	30 ppm/ $\text{V}\cdot\mu\text{m}^{-1}$

employs electrically loaded IDTs. Therefore, the cross sensitivities for other effects to the sensor can be minimized by suitable packaging and application of external sensor elements with well-known and specified properties. The applied SAW devices are named indirectly affected SAW sensors or SAW transponder sensors.

One port (IDT) of the device sketched in Fig. 1 is connected to the antenna; the reflector  $R_2$  is electrically loaded by an external impedance  $Z_{\text{load}}$ . The reflector is modeled as a device with two acoustical (1), (2) and one electrical (3) port.

The acoustic reflectivity  $P_{11}$  of  $R_2$  as a function of a complex termination impedance  $Z_{\text{load}}$  at its electrical port is given in (2) [15] in the well-known  $P$ -matrix formalism, where  $P_{11}^{\text{sc}}$  is the reflectivity for electrical short. For a split finger IDT, it is approximately zero.

$$P_{11}(Z_{\text{load}}) = P_{11}^{\text{sc}} + \frac{2 \cdot P_{13}^2}{P_{33} + \frac{1}{Z_{\text{load}}}} \quad (2)$$

The acoustic reflection coefficient is a complex parameter; the according signal of the sensor response is affected in magnitude and phase. In Fig. 2, the complex acoustic reflection coefficient is drawn for resistive, inductive, and capacitive load. To achieve sensor capability with maximum dynamic,  $Z_{\text{load}}$  is a serial resonance circuit. The measurand affects at least one element of this circuit. The resolution is determined by the external sensor device and by the nonlinear relation in (2). A measurand resolution  $< 1\%$  of full scale is achieved in worst case.

To double the sensitivity of this type of sensor, a third reflector  $R_3$  with maximum acoustic reflectivity is arranged in line with  $R_2$ . The SAW propagates from the IDT to  $R_3$  and back again and passes  $R_2$  two times. Here,

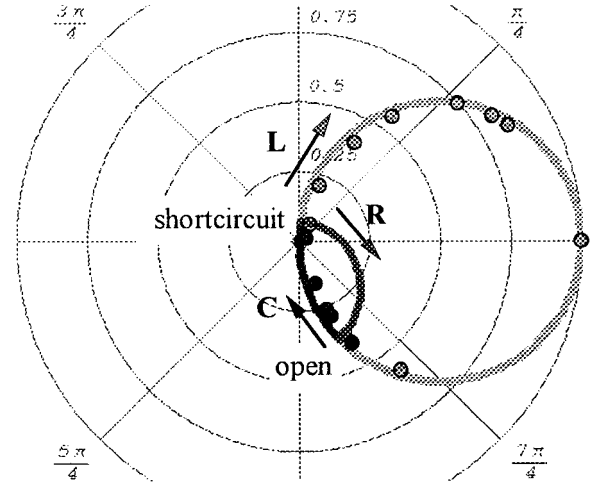


Fig. 2. Acoustic reflection coefficient of a splitfinger IDT as a function of its electrical load.

it is affected in magnitude and phase according to the acoustic transmission coefficient  $P_{12} = P_{21}$  (because of the reciprocity of the scattering matrix  $S$  and the unambiguous relationship between  $S$  and  $P$  matrix). It is found to be [15]:

$$P_{21}(Z_{\text{load}}) = P_{21}^{\text{open}} - \frac{2 \cdot P_{23}^2}{P_{33} + \frac{1}{Z_{\text{load}}}} \quad (3)$$

Monitoring the amplitude ratio or the phase difference of the response signals originating from  $R_1$  and  $R_3$  yields twice the effect compared with the modulation of reflectivity of  $R_2$  mentioned previously.

The advantage of this new indirectly affected SAW DL sensors is the separation between time delaying RF transponder and actual sensor. The SAW chip can be enclosed in a stable package, insulated from mechanical and chemical deterioration.

Applying SAW resonators (SAWR), the high-Q SAW device is excited by an RF signal. After switching off the stimulus signal, the high-Q resonator transmits a decaying signal at its resonance frequency that can be evaluated for several microseconds [17].

The Fourier transform of this signal yields an exponential spectrum that is almost symmetrical to the center frequency. SAWR can be applied as single or multiple resonant devices. In analogy to the reflectors of a coded

DL in time domain, for identification purposes, multiple resonance frequency devices are used as data words in frequency domain.

The resonance frequency of a SAW is determined by the distance between the reflector's electrodes  $d = \lambda_{\text{SAW}}/2$ . If  $d$  and  $\lambda_{\text{SAW}} = v_{\text{SAW}}/f = v_{\text{SAW}} \cdot T_p$ , respectively, are affected, the resonance frequency is shifted for

$$\begin{aligned} \Delta f &= f_{p,y} - f_{p,0} = \frac{1}{T_{p,y}} - \frac{1}{T_{p,0}} \\ &= \frac{S_T^y \cdot y}{T_{p,0} \cdot (1 + S_T^y \cdot y)} = \frac{S_T^y \cdot y}{T_{p,y}}. \end{aligned} \quad (4)$$

SAW sensors are totally passive and contain neither active elements nor batteries. Because no semiconductors are applied, the sensors withstand a high rate of radiation and a powerful electromagnetic interference (EMI) up to the power endurance of the device. A damage occurs if the electric field strength within the IDT exceeds the breakthrough threshold between the IDT fingers. For 433-MHz devices, this upper limit is at a few volts rms. With suitable packaging, the sensors are applicable in dusty environments with high mechanical load. Taking proper materials for manufacturing, the devices are capable of withstanding severe environmental conditions.

### III. RADIO REQUEST OF SAW SENSORS

Regardless of which type of SAW radio sensor is used, the sensor responds with an RF signal derived from the radio request signal by a linear (amplitude, time) distortion. A wireless one-port response measurement has to be performed. Similar to RADAR systems and also vector network analyzers (VNA), the receiver usually is located near the transmitter or included in the same set. Therefore, coherent detection is feasible.

#### A. Radio Request Methods

For the linear passive SAW sensors, TDD for separation of the request and the response signal is used, employing the energy storage in the SAW. The radio interrogation evaluation can be done in time (RADAR) and frequency (VNA) domain, we divide into

- TDS (wideband or full band sampling) and
- FDS (narrowband or partial band sampling).

1. *Time Domain Sampling:* For TDS, resolution in time is achieved by a radio request, covering the total system bandwidth at once (full band). To cover a sensor bandwidth  $B_{\text{sensor}}$ , it is trivial that the duration of the radio request signal  $T_{\text{signal,TDS}}$  for nonspread spectrum signals be

$$T_{\text{signal,TDS}} \leq \frac{1}{2 \cdot B_{\text{sensor}}}. \quad (5)$$

Utilizing spread spectrum signals with a bandwidth  $B_{\text{SS}}$  and a duration  $T_{\text{SS}}$ , an enhancement of signal energy of up to the process gain  $B_{\text{SS}} \cdot T_{\text{SS}}$  and the same improvement of

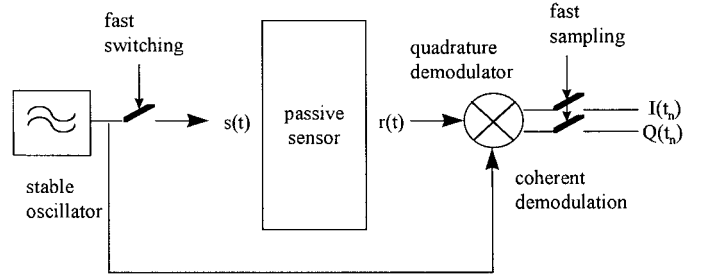


Fig. 3. TDS transmitter and receiver.

the system's performance is achieved. Here,  $T_{\text{SS}}$  is limited by the SAW storage time to a few microseconds. With the bandwidth of actual SAW sensors of 10 MHz (for example), the achievable gain is up to 20 dB. Each radio request signal causes one (single SAWR) or a number of (DL) response signals. A wideband detection of the response signal is performed in the receiver. A time delay or the response frequency is detected from the received signals. For the request of SAW DL, the bandwidth has to be high enough to distinguish the response signals, to make them orthogonal in time. Requesting resonators, the signal's bandwidth has to cover the bandwidth of the resonator (or the total bandwidth of the resonators in a multiple resonator device) to excite all resonance frequencies of the assembly. Choosing the bandwidth of radio request too high means a needless waste of energy.

With TDS, the whole sensor response can be recorded in one radio request cycle, i.e., TDS is a single scan measurement method. The energy contents  $E_{\text{TDS},0}$  of one request is low

$$E_{\text{TDS},0} = \int_{t=0}^T P dt \quad (6)$$

with the bandwidth  $B \approx 2/T$  and the signal power  $P$  simplified to  $P \cdot T$  for bursts with constant power  $P$  and duration  $T \approx 1/2B$ .

Fig. 3 shows the principle of a TDS system.

Coherent measurement is performed by coherent quadrature demodulation of the received signal  $r(t)$  referenced to the stable oscillator utilized in the transmitter section. The baseband signal, then, is  $M$  times sampled at the sample times  $t_m$ . The sampling bandwidth has to be chosen properly, so that the convolution of the signal with the sampling window does not disturb the results. Of course, the sampling theorem applies, and the sampling has to be performed with at least twice the bandwidth of the baseband signals.

The sampling delivers a two column table of inphase ( $I$ , column 1) and quadrature phase ( $Q$ , column 2) components of the received signal versus time (row number  $m$ ). This corresponds to the discrete time response (e.g., burst response) of the sensor to the request signal  $s(t)$  (e.g., a burst). Magnitude and phase versus time are evaluated easily. Differential phase and amplitude measurements for different reflectors are calculated from these results.

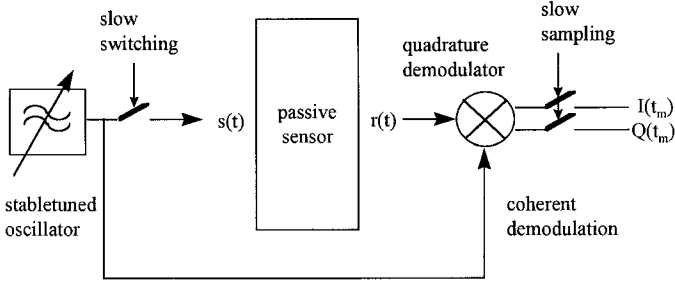


Fig. 4. FDS transmitter and receiver principle.

TDS provides fast access to the sensor information with low energy contents. It requires high speed RF switches in the transmitter and fast data acquisition in the receiver.

*2. Frequency Domain Sampling:* FDS or partial band sampling means scanning of the total bandwidth  $B$  step by step in the frequency domain. Similar to the way it is performed in a VNWA, the sensor response is measured for a number  $M$  of scans at center frequencies  $f_m$ . To achieve high resolution, the bandwidth  $B_{\text{res}}$  of one step must be small, requiring a relatively long duration of the radio signal and enhancing the total measurement time as well as the total energy used for detection. The duration of one radio request signal  $T_{\text{signal, FDS}}$  at one frequency is

$$T_{\text{signal, FDS}} \geq \frac{1}{2 \cdot B_{\text{res}}} \quad (7)$$

with the resolution bandwidth  $B_{\text{res}}$

$$B_{\text{res}} = \frac{B}{M}. \quad (8)$$

In Fig. 4, an FDS system is sketched. As for the TDS system (Fig. 3), the RF local oscillator signals in the receiver section can be derived from the transmitter oscillator. FDS is a multiscan measurement. To achieve the information of a number of  $M$  points in time,  $M$  frequencies have to be scanned by radio interrogation. The total measurement in minimum lasts  $M$  times the minimum measurement cycle of TDS.

The usually used radio request method for passive SAW sensors is TDS with wideband signals with a transmitted energy contents of  $E_0 = 1$  nWs to 20  $\mu$ Ws for high speed, low range, and low cost applications of DL sensors and SAWR.

Stepped FDS methods employ inverse fast Fourier transform (IFFT) algorithms in the receiver. A total (multiscan) energy of up to 300  $\mu$ Ws is transmitted in  $M$  (e.g.,  $M = 32$ ) request signals. The systems are employed for precise long distance interrogation of DL sensor. Further, analog integrating methods such as the Gated Phase Locked Loop are operated for SAWR applications [17].

### B. Parameter Measurement

The received analog signal is sampled and digitized. Employing TDS, the sensor's time response is stored in

an array as real and imaginary part or magnitude and phase of the samples. Assuming a coherent system, the phase is referenced to a clock that is used to generate all frequencies in the interrogation system.

FDS generates a complex array with real and imaginary part, or magnitude and phase, respectively, of the sensor's frequency response. The row index is the frequency of measurement or the concerning number of the equally spaced frequency steps. Utilizing a discrete Fourier transform algorithm, time sampling results can be converted to frequency and vice versa.

For measurement, from these arrays, the parameters time and frequency have to be measured or estimated, respectively, in the receiver. Methods of measurement as currently applied are discussed here.

*1. Measurement of Time:* The time delay  $\Delta\tau$  between two impulses in baseband or bandpass range can be done differently. One method employs measurements based on the envelope function of the signal; another utilizes zero crossings, or phase, respectively.

The most important and commonly utilized method is the phase measurement in coherent systems. The received response is coherently converted into the orthogonal base system of the transmitter's reference. The detector yields the inphase ( $I$ ) and the quadrature phase ( $Q$ ) component of the input. The phase of the received signal relative to the reference is calculated from

$$\varphi(t) = \arctan\left(\frac{Q(t)}{I(t)}\right). \quad (9)$$

Applying differential measurements, a change of absolute phase caused by a changing radio channel is compensated. A  $2\pi$  phase shift corresponds to a time shift of one period length of the burst center frequency. For a 433-MHz RF frequency, the period length is approximately 2.3 ns. A phase resolution of only  $\pi/6$  yields a resolution in time of 0.19 ns. The time measurement by phase detection is the most common method employed in today's SAW radio sensor systems.

*2. Measurement of Frequency:* In actual radio sensor systems, the measurement of frequency, e.g., of the decaying SAWR response, is done by several methods. From TDS, the received signal is sampled and digitally processed utilizing FFT, parameter fitting, or by zero crossing counting. An analog solution employs the gated PLL principle [17]. It is important to note that the frequency of the short signals can be measured with an uncertainty in frequency only. So, e.g., the response of a decaying resonator has a spectrum with exponential decay centered at the resonance. Employing FFT yields samples in frequency domain with a spacing  $\Delta f_{\text{FFT}}$  determined by the sample rate in time domain. The uncertainty is up to  $\Delta f_{\text{FFT}}/2$ .

*3. Measurement of Amplitude:* In passive radio sensor applications, analog amplitude information is used rarely because it is strongly affected by the radio transmission.

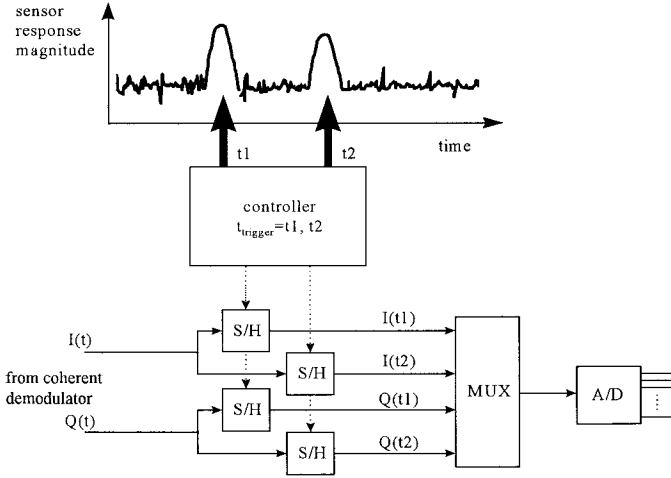


Fig. 5. TDS sampling on demand. S/H = Sample hold; MUX = multiplexer for ADC.

It only is applied for the measurement of the difference between the affected and the reference reflector employing indirectly affected SAW transponders.

### C. Data Reduction

Data reduction and interpolation methods are applied to simplify the baseband processing system.

1. *Reduced TDS*: For DL interrogation, magnitude and phase have to be measured at a few discrete sample points in time only. For data reduction, an asynchronous sampling is applied utilizing individually triggered sample/hold circuits. As sketched in Fig. 5, for a two burst response, only four digital data words have to be processed off-line. A low cost microcontroller can be utilized.

2. *Reduced FDS*: Data reduction in frequency domain utilizes FDS at only a reduced number of frequencies and a model based parameter estimation of the frequency domain sensor reflectivity. This new method has been presented and investigated in [18]. A DL with two reflectors is modeled as a two path radio transmission channel with delays  $\tau_1$  and  $\tau_2$ . The parameters delay difference  $\tau_2 - \tau_1$ ; amplitude ratio  $a_2/a_1$  and phase difference  $\varphi_2 - \varphi_1$  are calculated from only three samples in frequency domain.

### D. Enhancement of Signal's Energy

As in RADAR systems, coherent integration is applied in radio interrogation of passive sensors. The average of the received signals from  $N$  interrogation cycles is

$$r_N(t) = \frac{1}{N} \cdot \left( N \cdot r(t) + \sum_{k=1}^N n_k(t) \right). \quad (10)$$

The received response signals  $r(t)$  are assumed to be constant in magnitude and phase during integration. In practical use, the complex valued samples  $I$  and  $Q$  of the signal's amplitude  $r_k(t)$  of different interrogation cycles are

summed up and divided by  $N$ . The mean signal amplitude  $r_N(t) = r(t)$ , and, therefore, the mean signal power is not affected by the linear averaging.

Because of the linear process, there is no cross-correlation between signal and noise; they are still summed additively. Assuming additive white Gaussian noise (AWGN), the cross-correlation between different noise samples vanishes. Thus, the normalized noise power  $P_n$  after averaging is

$$P_n = \frac{1}{N^2} \cdot E \left\{ \left( \sum_{k=1}^N n_k(t) \right)^2 \right\} \\ = \frac{1}{N^2} \cdot \sum_{k=1}^N E \left\{ (n_k(t))^2 \right\}. \quad (11)$$

With  $E\{\dots\}$  the expectation value and  $\overline{(n_k(t))^2}$  the mean power of the stochastic noise, the previously mentioned averaging yields a mean noise power  $P_n$

$$P_n = \frac{1}{N^2} \cdot \sum_{k=1}^N \overline{(n_k(t))^2} = \frac{\overline{(n_k(t))^2}}{N}. \quad (12)$$

The noise power is reduced by coherent integration; the signal to noise power ratio SNR is increased by a factor  $N$ . In other words, the total energy for signal detection is enhanced by a factor of  $N$  with a constant AWGN power.

Coherent integration is applicable for signal to interference ratio (SIR) enhancement also, if no correlation of signal and interference signal exists. Feedthrough effects originated from local oscillators within the radio request system cannot be coped with.

Nonlinear signal handling in the receiver causes an irreversible correlation between signal and noise terms. Then, above a threshold SNR, less effective nonlinear integration measures, e.g., post detection integration, can be applied. The simplest post detection integration is a majority decision considering the results of  $N$  measurement cycles. For integration, a stationary measurand was assumed. For actual measurements, this assumption is violated often.

A continuously increasing phase shift  $\Delta\gamma$  between the  $N$  samples with amplitude  $a$  yields a total phase error of  $\pm N \cdot \Delta\gamma/2$ . For small  $\Delta\gamma$ , the total amplitude  $A$  is

$$A = a \cdot \sum_{n=1}^N \cos \left[ \frac{n \cdot \gamma}{2} \right] \quad (13)$$

and, with mathematical conversion,

$$A = a \cdot \frac{\sin \left[ \left( \frac{1}{2} + N \right) \cdot \frac{\gamma}{2} \right]}{\sin \left( \frac{\gamma}{4} \right)}. \quad (14)$$

Then, the relative amplitude error is

$$\frac{N \cdot a - A}{N \cdot a}. \quad (15)$$

Apart from nonstationary measurands, an origin of such a phase shift is the Doppler scaling caused by a fast moving sensor. Because it is very small for the used frequency

ranges, it actually has no importance for the measurements. Further, for fast moving sensors, the range of radio contact and, therefore, the time interval of radio request is small because of the radio signal attenuation ( $d^p$  law).

### E. Multiple Access

In the same manner that the radio request signal and the sensor response are separated on the radio channel for transmission (TDD, FDD, ...), the response signals of different sensors can be distinguished for individual access. Because the SAW devices are linear, a division in frequency is feasible for high- $Q$  resonators only. For DL, the most usual methods are space division multiple access (SDMA) and time division multiple access (TDMA), utilizing the known energy storage time.

SDMA is suitable; the sensors and, e.g., the work pieces to monitor, are allowed to move in certain ways and with sufficient distance to the next one. Then, because of the beam width of the antennas and because of the  $d^p$  propagation attenuation, the amplitude of the selected response is large enough to provide a sufficient SIR with the interference from the others. For this application, gain controlled and logarithmic amplifiers have to be limited in their dynamic range. The error caused by interference originating from unwanted sensor response can be estimated similar to other interference (see Section V, A5). SAW sensors with SDMA mainly are applied to identification purposes, where the amplitude and phase error effects are less significant, e.g., it is applied for the Norway road pricing system KOFRI [12]. The advantage of SDMA is that the whole code family can be exploited with the exception of a start and stop bit. With a 32-bit code and on/off keying,  $2^{30}$  sensors can be distinguished.

For SAW DL sensor purposes, usually time division TDMA is applied. The response of the sensors within the range of an interrogation unit are separated, interleaving them in time in individual time slots. Two-bit DLs, e.g., sensor  $u = 1, 2, \dots$ , respond in the time slots  $u$  and  $u + v$ , with a constant offset  $v$ .

The advantage of this method is that, neglecting the sidelobes in time originated by the bandpass filters, interference from the response signals of other sensors is minimized. A near far problem is almost not occurring; the response signals do not have to be received with almost equal signal strength. The time slots have to be wide enough that the response signals stay within despite the shifts caused by the measurand (also see Section IV, A). Multiple access by code division (CDMA) is difficult due to a severe near far effect because of the  $d^p$  RF attenuation ( $p \geq 4$ ) for passive transponders. Some work has been done for SAW sensor CDMA in our laboratory; results have been published in [19]–[21]. Best results have been found by a combination of CDMA with a TDMA. There, the code selective addressed sensor responds in a characteristic time slot; the interference from the others can be minimized by proper choice of code and timing [22]. To find the measurand, a kind of Wavelet transform

is applied with the available codes as mother-Wavelets and the overlapping received response signals as a sum of these signals scaled in time.

## IV. RADIO TRANSMISSION

The propagation via the radio channel mainly is affected by the following:

- signal attenuation because of the distance between the antennas in the far field. [The far field approximation is valid at a distance larger than  $r_2$ , with  $r_2 = 2D_0^2/\lambda$ , with the maximum geometrical extension of the antenna  $D_0$  and the wavelength  $\lambda = c/f$  with  $c$  equal to the velocity of electromagnetic wave propagation, velocity of light, and  $f$  equal to the RF frequency. For small antennas  $D_0 \ll \lambda$ , commonly used for passive sensors, the near field reaches up to  $r_1 \gg \lambda/2\pi$ . There, the (“free space,”  $p = 2$ ) attenuation of an RF signal unidirectionally transmitted from one isotropic antenna to another is

$$a_{\text{free\_space}} = \left( \frac{4 \cdot \pi \cdot d}{\lambda} \right)^p. \quad (16)$$

Actual exponents  $p$  in mobile communication engineering are 3 to 4 due to ground effects, etc. For passive transponders, because the channel is passed two times,  $p$  has to be doubled.]

- slow fading caused by obstructed propagation, shadowing, etc.
- frequency selective and Rayleigh fading caused by multipath propagation and interfering signal components
- thermal and man made noise
- co-channel interference originated by other (ISM band) RF systems.

As an example, Fig. 6 shows the signal attenuation for a very short range radio channel ( $\lambda \approx 0.7$  m) between a radio request antenna under the fender of a car and the radio sensor inside the tire. The signal attenuation for this short range channel is characterized mainly by the geometrical position and the displacement of antennas and misadjustment of polarization. The distance  $r$  is 0.2 to 1.0 m. Small antennas have been used; although, because metallic parts of the car enlarge the effective antenna aperture, near field coupling is applied. The two graphs shown in Fig. 6 represent two different antenna positions.

For far field radio propagation, a movement of approximately one-tenth of the wavelength yields a totally changed scenario. The radio signal is transmitted via a number of channels. Multipath propagation occurs, characterized by statistical parameters comprehensively discussed by T.S. Rappaport [23]. Mean delay, mean excess delay, rms delay spread, and the maximum excess delay  $\{-x\text{dB}\}$  describe the channel in time domain. Typical delay spreads  $\sigma_\tau$  are a few microseconds for outdoor channels and up to 200 ns for indoor channels.

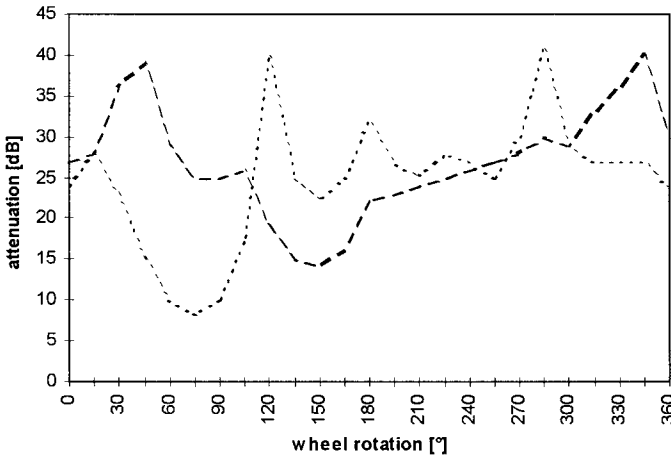


Fig. 6. Signal attenuation for the 433-MHz radio link vs. wheel rotation for two antenna positions.

In frequency domain, Doppler spread and coherence bandwidth  $B_c$  are utilized. Here,  $B_c$  gives a statistical measure of the range of frequencies over which the channel can be considered “flat.” This means that all spectral components within this bandwidth pass the channel with approximately equal attenuation and linear phase. Spectral components within  $B_c$  show correlation of amplitude fading; the fading for a flat multipath channel obeys a Rayleigh distribution. For a correlation coefficient of 0.5, Rappaport estimates the coherence bandwidth to be

$$B_c \approx \frac{1}{5 \cdot \sigma_\tau}. \quad (17)$$

If the signal bandwidth is smaller than  $B_c$ , fast Rayleigh fading occurs. Otherwise, multiple echoes are detected. For medium range (a few meters) industrial sensor interrogation radio channels, we found a mean excess delay of approximately 20 ns, a rms delay spread of approximately 20 ns, and an excess delay spread (for an amplitude dynamic of 20 dB) of 75 ns with a standard deviation of < 20%.

Within the response time of a few microseconds, the linear, narrowband radio channel for the same frequency utilized in down- and uplink is assumed to be stationary. Radio signals interrogating passive sensors pass the same channel over the same antennas two times; all effects occur twice. Therefore, the path loss is squared, doubled in decibels. The total impulse response is calculated from the autoconvolution of the unidirectional channel impulse response. A worst case estimation yields a doubling of delay and delay spread, and the coherence bandwidth is halved.

#### A. System Design with Respect to the Radio Channel's Properties

From the average parameters of the radio channel, the basic design rules for the radio sensors and the radio interrogation system can be derived.

The doubled delay spread of the channel determines the minimum of the spacing in time of neighbored reflectors of

SAW DL sensors (Fig. 1) or for TDMA slots for different DL sensors. Therefore, this limits the number of reflectors and sensors (with TDMA) for a given maximum substrate length.

On a substrate with a given TK, the earliest time position of the  $n$ th reflector  $t(x_n)$  to avoid interference of adjacent reflected signals is

$$t(x_n) = (1 + \text{TK} \cdot \Delta\vartheta_{\max}) \cdot t(x_{n-1}) + \left( 2 \cdot \text{eds}\{x\text{dB}\} + \frac{2}{B_{\text{RF}}} \right). \quad (18)$$

For worst case estimation, to the position of the  $(n-1)$ th reflector for maximum temperature shift  $\Delta\vartheta_{\max}$ , the doubled excess delay spread  $\text{eds}\{x\text{dB}\}$  and the pulse width  $2/B_{\text{RF}}$  have to be added.

Mathematical conversion yields

$$t(x_n) = (1 + \text{TK} \cdot \Delta\vartheta_{\max})^n \cdot t(x_0) - \frac{1 - (1 + \text{TK} \cdot \Delta\vartheta_{\max})^n}{\text{TK} \cdot \Delta\vartheta_{\max}} \cdot \left( 2 \cdot \text{eds}\{x\text{dB}\} + \frac{2}{B_{\text{RF}}} \right). \quad (19)$$

From (18) and (19), the maximum substrate length, the number of sensors interrogated simultaneously, the RF bandwidth required, or the temperature range allowed for operation can be extracted from the other parameters.

This estimation also applies to the number of on/off set bits of an ID sensor. A LiNbO<sub>3</sub> ID tag with a total delay of 10  $\mu\text{s}$  and a temperature range of 50 K can utilize in maximum 6 bits, if it is interrogated by a 433-MHz radio signal with the allowed ISM bandwidth. A 10-MHz bandwidth, e.g., in the 2.45-GHz ISM band allows 14 bits for ID or sensor applications with a 10- $\mu\text{s}$  SAW DL (2 · 15 mm SAW propagation length, approximately 20 mm substrate length). Applying TDMA with 2-bit DLs and pairs of reflectors interleaved in time over 14 possible time slots, up to 7 SAW sensors can be requested simultaneously.

In Fig. 7, a link budget for an actual SAW RF ID system is drawn for an outdoor entrance control application. The system operates in the 433-MHz ISM band; the distance range is approximately 3 m, the unidirectional propagation attenuation was assumed to obey a  $d^2$  law, and no margin for fading was considered. The antennas employed are electrically shortened dipoles with a total gain (including misadjustment) of approximately 0 dBi (relative to isotropic antenna). The noise power to be considered is the sum in decibels of thermal and man-made noise and the receiver's noise figure. The SNR at the receiver output (at the detector, where the amplitude or phase is measured) determines measurement error rate and will be subject to further investigations subsequently.

## V. MEASUREMENT UNCERTAINTY

### A. Sensitivity, Resolution, and Accuracy

The sensitivity of a sensor usually is defined as the change of the sensor readout because of the effect of cer-

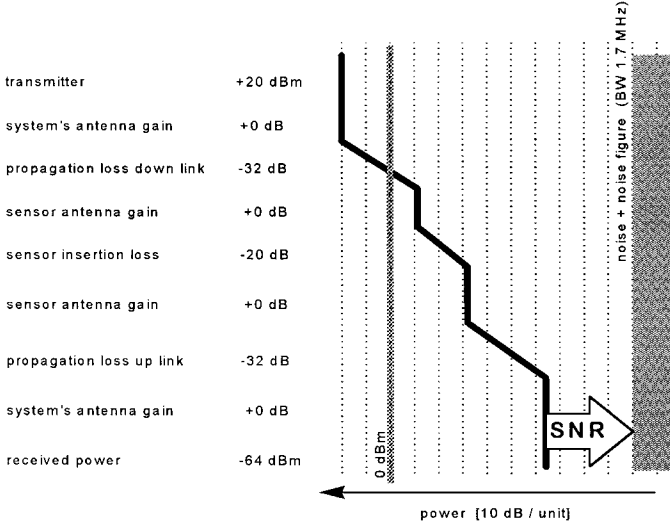


Fig. 7. Link budget for an outdoor short range ID application.

tain parameters. Acoustic delay in a SAW device depends on the acoustic propagation velocity and the propagation distance. Every effect to the SAW device, affecting one or both, respectively, will yield a variation of delay time, resonance frequency, etc. The sensitivity of delay  $T$ , e.g., for temperature  $\vartheta$ ,  $S_T^\vartheta$  includes the assumption, that all other effects are kept constant. Examples of the sensitivity of directly affected SAW sensors are given in Tables I and II. Applying the indirectly affected SAW transponder sensors some tens of percent of nonlinear full range amplitude variation are achieved for a change of the external impedance by a factor of two.

Resolution is the minimum detectable change of the measurand in the measurement system's (in most cases digital) readout. For SAW DL sensors, the resolution of the measurement is enhanced by phase discrimination. Evaluation of delay from the response signal's envelope only yields a resolution of a few nanoseconds. Similar to results mentioned previously, with phase evaluation, a small time delay corresponding to a phase shift can be detected with a much higher sensitivity (also see Section III, B2). A resolution of 1 degree for phase detection at a 1-GHz RF frequency corresponds to a time resolution of  $\Delta T_{\min} = 1 / (360 \cdot f_0)$ ,  $< 3$  ps. The relative resolution  $R_{\text{rel}}$  of the measurement, the ratio of total delay to the smallest delay to discriminate, is  $R_{\text{rel}} = T_{\text{total}} / \Delta T_{\min}$ . For a 3- $\mu\text{s}$  sensor delay interval, the relative resolution is enhanced from  $10^{-3}$  to  $10^{-6}$ , replacing time delay by phase measurement. The actual achieved resolution for the indirectly affected SAW transponders is better than 1% in worst case. Resolution of measurement often is mixed up with accuracy:

The accuracy is the fidelity of the system's readout to the actual measurand. In actual systems, errors occur because of the sensor itself, because of the signal processing, and because of external effects from the radio propagation as well as noise and interference.

### B. Measurement Errors

The most important measurement errors occurring in SAW sensor systems are listed in Table III. In the subsequent investigations, the error is calculated for time parameters. Employing frequency measurement, the relative frequency error  $\Delta f / f$  can be calculated from the phase error  $\Delta\varphi$ . Measurement of one period length is afflicted with an error in frequency of  $\Delta\varphi / 2\pi$ . If the phase is unambiguous, the number of periods is counted for a time interval  $T_m$ , and the relative frequency error is calculated from

$$\frac{\Delta f}{f} = \frac{\Delta\varphi}{2\pi} \cdot \frac{1}{T_m \cdot f}. \quad (20)$$

1. *Manufacturing and Aging:* In fabrication, the tolerances are given to be up to 100 ppm =  $10^{-4}$  for low-cost SAW mass products [24], representing the accuracy limit for the SAW sensors without calibration. For resonant devices, total aging remains smaller than  $\pm 50$  ppm. For DL, aging only depends on the almost neglectable aging of the crystal substrate and is not specified.

2. *Bandwidth:* The bandwidth of measurement is the maximum bandwidth of the dynamic measurand allowed for admissible errors. The total measurement transfer function includes the transfer functions of the environment, the sensor, the radio transmission, and the signal processing. The environment includes the system, converting the measurand into the effect on the sensor. This environment can be a membrane for pressure measurement, it also can be a surface layer for gas adsorption. For temperature measurements, because of the thermal energy storage capability, the total sensor system commonly is a low pass system for the temperature with one or more cut-off frequencies. The bandwidth is limited maximally by a few hertz.

On the other hand, for the directly mechanically affected SAW sensors, the front end usually is a damped resonant system with a mechanical resonance of up to several kilohertz. The transfer function of the signal processing also depends on the principle applied. Usually the measurand is calculated from a time delay or by a frequency measurement, lasting a time interval. Within this time, an integral value of the measurand is collected. As shown in [25], the maximum error occurs at zero crossing of the measurand. With  $\sin(x) \approx x$  for small  $x$ , the error increases up to 1% if the measurement interval  $\Delta T$  is up to 1% of the measurand's period  $1 / f_{\text{meas}}$ . A tradeoff between resolution and bandwidth has to be found, e.g., a 3- $\mu\text{s}$  DL with a resolution of up to  $10^{-6}$  can be operated up to a frequency of  $f_{\text{meas}} \approx 3$  kHz to keep the additional bandwidth error because of the measurement  $< 1\%$ .

In contrast to directly affected SAW sensors, being a part of the front end, indirectly affected SAW transponders belong to the task group of radio transmission. The reflected signal is measured almost instantaneously relative to an unloaded reference reflector  $R_1$  (see Fig. 1). No integration for a long period is performed. Here, the

TABLE III  
DETERMINISTIC AND STOCHASTIC ERRORS FOR RADIO REQUEST OF PASSIVE SAW SENSORS.

Origin	Effect	Result
Sensor	manufacturing aging bandwidth	deviation of delay or frequency
System	tuning - gain (includes S/H hold drift, ...) - phase orthogonality phase noise ADC bandwidth	deviation of amplitude and phase phase and amplitude error  depending on ADC resolution assumed to be sufficiently wide
Radio channel	noise, interference	phase and amplitude error

upper bandwidth limit is given by the mechanical length and, therefore, by the acoustic bandwidth of the IDTs and by the electrical bandwidth of the impedance matching circuits. A minimum time delay (also see Section IV, A) between the reflected response is required to avoid intersymbol interference. This minimum distance in time, and, therefore, the required RF bandwidth (BWR<sub>F</sub>) for operation, is much more limited by the governmental regulations than by the SAW RF bandwidth for highly reflective devices. However, by decreasing the time of integration from microseconds (for the directly affected DL) to a few tens of nanoseconds for SAW transponders, simultaneously, the error caused by a dynamic measurand is decreased or the permissible measurand's bandwidth is increased, respectively.

The measurand is sampled every radio interrogation cycle. A minimum interrogation cycle with differential measurement lasts one radio request and two sensor response impulses, corresponding to  $3/BW_{RF}$ . According to Shannon's sampling theorem, the sampling frequency (frequency of interrogation) has to be higher than twice the highest spectral component of the measurand. Considering the transmit/receive cycles, the maximum bandwidth of the measurand must be smaller than the sixth part of the RF bandwidth.

To reduce the errors caused by integration of the sensor effect, the measurand's bandwidth limit is set to approximately  $BW_{RF}/10$ . A measurand (converted to an impedance for an indirectly affected SAW transponder) with a bandwidth of up to a few megahertz can be measured wirelessly [28]. In actual applications for the measurement of mechanical parameters, the external conventional sensors, providing the variable impedance, limit the bandwidth to a much narrower range.

*3. Receiver Tuning:* In the receiver, coherent detection is performed, causing further errors. The base vector signals, assumed to be orthogonal, that the received signal is multiplied by have a deviation  $\gamma$  from exact orthogonality. The amplification and A/D conversion of the base-band signals are not exactly equal, but differ by a factor  $b/a$  ( $I' = I \cdot a$ ,  $Q' = Q \cdot b$ ). Both,  $\gamma$  and  $b/a \neq 1$ , cause er-

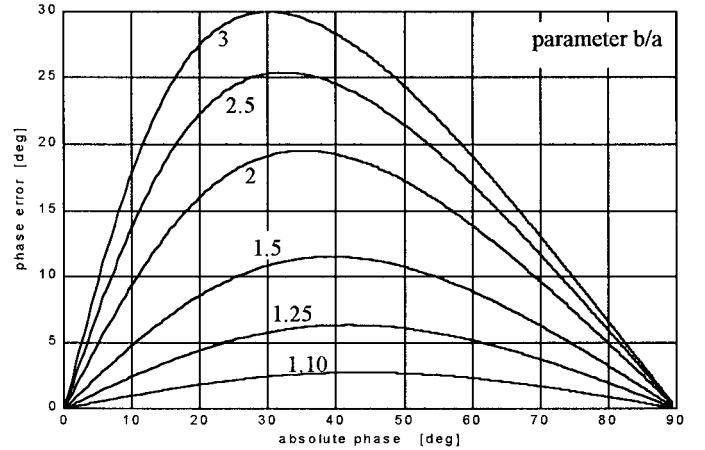


Fig. 8. Phase error  $\Delta\varphi_{b/a}$  caused by different base band gain vs. absolute phase, parameter  $b/a$ .

rors in phase ( $\Delta\varphi$ ) and amplitude ( $V'/V$ ).

$$\Delta\varphi_{b/a} = \arctan \left\{ \frac{B \cdot Q}{a \cdot I} \right\} - \arctan \left\{ \frac{Q}{I} \right\} \quad (21)$$

$$V'/V|_{b/a} = \sqrt{\left(\frac{b}{a}\right)^2 \cdot \sin^2 \varphi + \cos^2 \varphi} \quad (22)$$

$$\Delta\varphi_\gamma = \arctan \left\{ \frac{\cos(\pi/2 - \varphi - \gamma)}{\cos(\varphi)} \right\} - \varphi \quad (23)$$

$$V'/V|_\gamma = \sqrt{\cos^2(\varphi) + \cos^2(\pi/2 - \varphi - \gamma)} \quad (24)$$

The resulting errors have been calculated, and the results are drawn in Fig. 8, 9, 10, and 11.

*4. Phase Noise:* The oscillators used for signal generation and coherent detection are afflicted with phase noise. Because a multiplication is performed, the phase errors are considered only. For description of phase noise in frequency domain, the single sideband noise density is used because it can be measured easily. Another description calculated from  $S_\Theta(f)$  is the Allan variance, the mean frequency offset for samples spaced in time by  $\tau$  [26]. The local oscillators (LO) in transmitter and receiver are assumed to be similar, and the total phase noise effect is doubled for estimation. Considering both frequency sidebands by a factor of two,

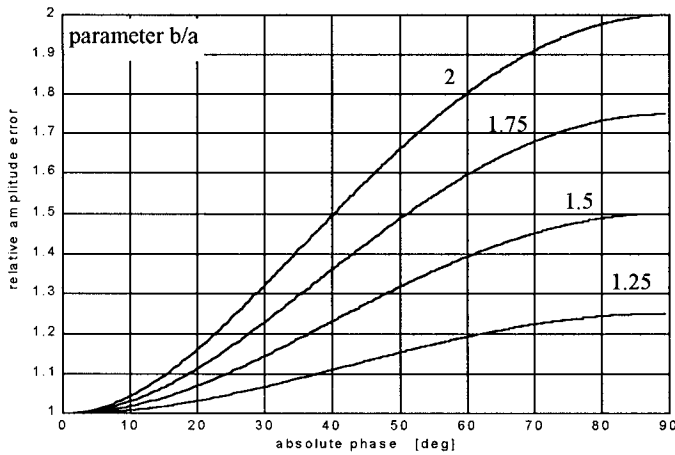


Fig. 9. Amplitude error  $V'/V|_{b/a}$  caused by different base band gain vs. absolute phase, parameter  $b/a$ .

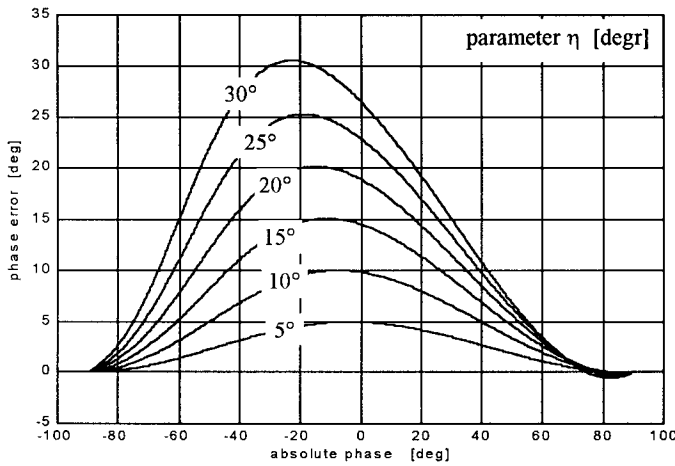


Fig. 10. Phase error  $\Delta\varphi_\gamma$  caused by the nonorthogonality of the reference, parameter  $\eta$ .

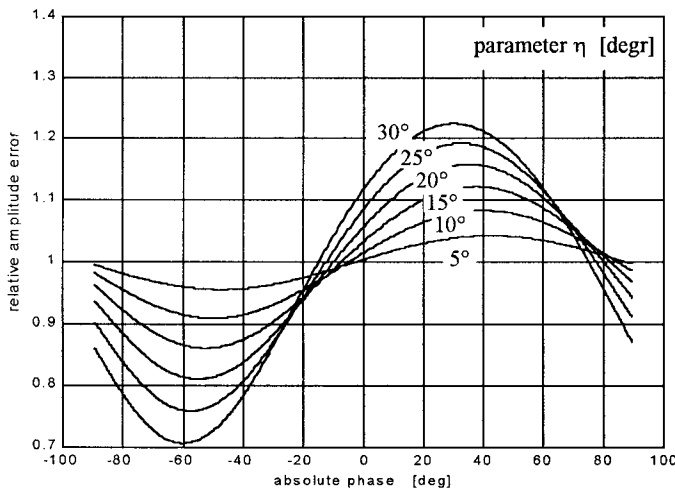


Fig. 11. Amplitude error  $V'/V_\gamma$  caused by the nonorthogonality of the reference, parameter  $\eta$ .

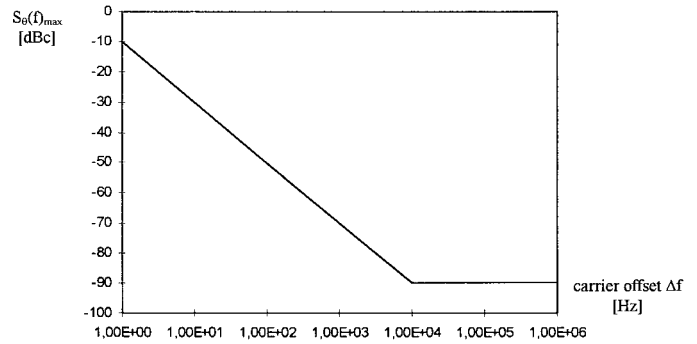


Fig. 12. Estimated phase noise mask for rms phase error of  $<1$  degree for a  $10\text{-}\mu\text{s}$  DL.

from [26], we find for the total mean squared phase noise  $\sigma_\theta^2$  in a bandwidth  $2 \cdot B$

$$\sigma_\theta^2 = 2 \cdot \int_0^B S_\theta(f) df. \tag{25}$$

The term  $\sigma_\theta$  in (25) is the rms phase deviation caused by the phase noise. Therefore, if the phase noise  $S_\theta(f)$  of the oscillators is known, the rms error of phase measurements in SAW sensor systems can be calculated. For all measurements of phase, the rms phase error just given occurs.

On the other hand, looking for a limit mask of the admissible phase noise of the oscillators for a maximum error, the spectrum is divided into subbands. The square root of the integral of the phase noise  $S_\theta(f)$  within the subbands represents the rms phase noise there. Employing differential measurements, the phase of one response signal is detected and, referenced to another component of the response, was received only a few microseconds  $\Delta T$  earlier or later. The phase noise contributes to an error, if it changes the absolute phase significantly within this time interval. Therefore, terms in a frequency subband, centered around the inverse time delay  $1/\Delta T$ , contribute directly; low frequency terms, corresponding to measurement at  $t \gg \Delta T$ , have a reduced effect on the results.

Therefore, we first will focus to the subband between 10 kHz and 1 MHz,  $\Delta T \approx 10 \mu\text{s}$ , and assume a flat spectral noise density there. The assumption that the maximum phase deviation caused by phase noise should be  $< 0.3$  degrees ( $5 \cdot 10^{-3}$  rad) yields a flat phase noise limit of approximately  $-90$  dBc for the mentioned subband for each of the oscillators. With decreasing frequency offset from the carrier, the phase noise effect decreases with 20 dB per decade; the noise power density may increase for this term. The total noise power is the sum of the power in the subbands; the total error is the sum of the rms errors.

The resulting limit mask for the phase noise density of each of the two oscillators in the radio request receiver is given in Fig. 12 for a total rms phase error of  $< 1$  degree. A comparison with the phase noise of a usually employed oscillator stabilized by a SAW resonator shows a margin of up to 10 dB. Therefore, the phase noise effect of these oscillators will not be critical for the measurement.

5. *Additive Noise and Interference Because of Radio Transmission:* During radio transmission, noise (assumed to be a white stochastic process with Gaussian probability density function of amplitude, AWGN) and interference from other RF radio systems are added. The power density of a white process is the autocorrelation function for a time shift of zero  $ACF(0)$ . For a Gaussian process, the double side noise power density can be calculated from the probability density function. It is equal to the variance  $\sigma^2$  [27]:

$$\sigma^2 = N_0/2. \quad (26)$$

The spectral noise density  $N_0$  of a resistor  $R$  at absolute temperature  $\vartheta$  is  $N_0 = 4 \cdot k \cdot \vartheta \cdot R$ , where  $k$  is the Boltzmann's constant. The noise power delivered from an antenna usually is calculated to be equal to the noise power of a resistor at the same temperature as the background the antenna is facing. The noise power  $N$  can be calculated from the product of power density  $N_0$  and two-sided bandwidth  $B$ :

$$N = (N_0/2) \cdot B.$$

In general, for an estimation of total noise power, man-made noise, originated from the electrical systems in our environment, has to be added. For frequencies at 400 MHz and above, it is neglectable. All noise power terms can be added if they are statistically independent.

The receiver noise is given by its noise figure NF, degrading the SNR at the input to the SNR at the detector where the amplitude or phase of the signal is measured and a mostly discrete decision is made. The noise figure of low-cost interrogation systems is about 3 to 10 dB. At the detector, the noise vector added to the received signal yields errors in phase and amplitude.

The amplitude error, the probability, that the measurement error caused by the AWGN exceeds  $w \cdot A_m$  with the signal's amplitude  $A_m$  can be written as

$$P_{\text{amplitude\_error}} = 2 \cdot Q \left\{ w \cdot \sqrt{\text{SNR}} \right\} \text{ for } w \geq 0. \quad (27)$$

The phase error caused by the AWGN is calculated very similarly to the investigation of the error of m-ary phase shift keying transmission. For small phase deviations caused by a large SNR, the probability that the phase error exceeds  $\Theta_r$  is [27]:

$$P_e \approx 2 \cdot Q \left\{ \sqrt{2 \frac{E_s}{N_0}} \cdot \sin \Theta_r \right\} \quad (28)$$

with the well-known  $Q$ -function  $Q\{z\} = \frac{1}{2} \left[ 1 - \text{erf} \left( \frac{z}{\sqrt{2}} \right) \right] = \frac{1}{2} \text{erfc} \left( \frac{z}{\sqrt{2}} \right)$ , the signal's energy  $E_s$ , and the noise density  $N_0$ . The results are drawn in Fig. 13 and 14.

For sensor applications, planned jamming is improbable. Radio interference usually originates in the interrogation system itself and by co-channel users (within the same

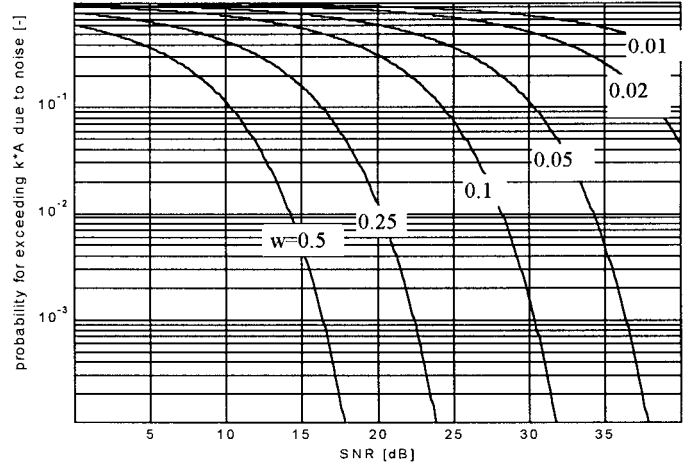


Fig. 13. Probability of measurement error vs. SNR for an error exceeding  $w \cdot A_m$  with parameter  $w$ .

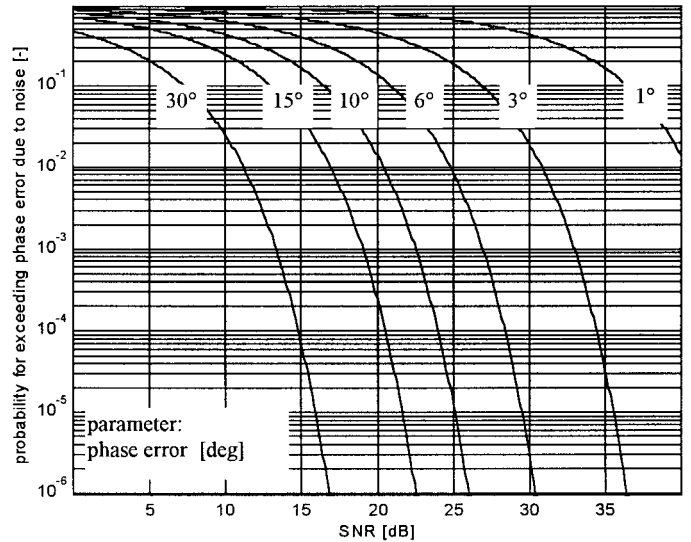


Fig. 14. Probability of phase error ( $\Delta\varphi > \theta_r$ ) is drawn vs. the SNR, with parameter  $\Theta_r$ .

ISM band). A feedthrough of local oscillators and response signals from other sensors cause coherent interference. This yields an interference signal  $i(t) = i_\tau(t) \cdot I_0 \cdot \cos(\omega t + \varphi)$  with a constant offset  $\varphi$  in phase to the reference signal, added to the received signal  $r(t) = r_\tau(t) \cdot R_0 \cdot \cos(\omega t + \phi)$  at the same frequency with  $i_\tau(t) = r_\tau(t) = 1$ , the SIR is the ratio of power levels  $R_0^2/I_0^2$ . In the receiver,  $i(t)$  interferes with the sensor response signals and provokes a fading depending on the measurand, affecting the phase  $\phi$ . Furthermore, because of the phase shift  $2 \cdot (2\pi \cdot d/\lambda)$  of the radio signal, the fading depends on the distance  $d$  between the interrogation antenna and the sensor. The amplitude varies between  $|I_0 - R_0|$  and  $|I_0 + R_0|$ . A phase error of up to  $\pm \arcsin \{I_0/R_0\}$  occurs. The phase error  $\Delta\varphi$  versus the SIR is plotted in Fig. 15. The amplitude error is  $\pm (I_0 + R_0)/R_0$ . A ratio of 40 dB for the SIR yields a maximum amplitude error of 1%.

Incoherent cochannel interference caused by other radio

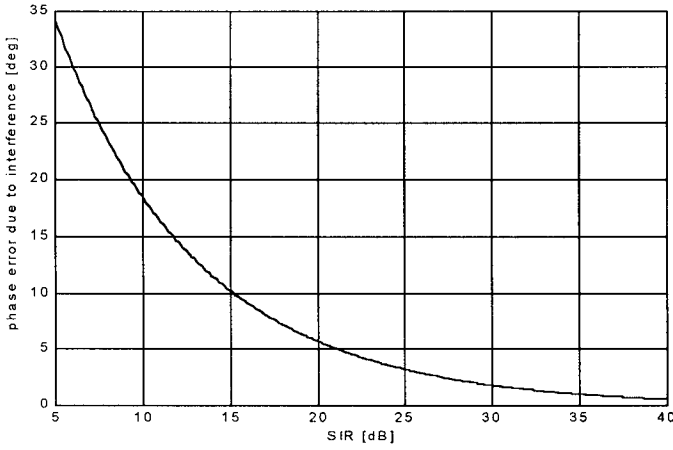


Fig. 15. Phase error caused by interference vs. SIR.

systems can be assumed to have a random phase. The estimations made for the coherent interferer with  $\varphi = 0$  and  $\varphi = \pi$  can be used as the maximum error here. On the other hand, the interference signal with random phase can be assumed to be a cyclostationary stochastic process. Then, the variance of the amplitude error, the squared rms interference, is  $(I_0/\sqrt{2})^2$ , and the expectation value of the phase error is  $\pm \arcsin \left\{ 2/\sqrt{\text{SIR}} \right\}$ .

6. *Digitization Error:* For digitization in an analog to digital converter (ADC), an amplitude error of up to 1/2 low significant bit voltage  $U_{\text{LSB}}$  cannot be avoided. The RMS error is

$$U_{e,\text{RMS}} = \frac{U_{\text{LSB}}}{\sqrt{12}}. \quad (29)$$

With an  $N$ -bit ADC, the RMS of a sinusoidal signal voltage  $U_{s,\text{RMS}}$  is

$$U_{s,\text{RMS}} = \frac{1}{\sqrt{2}} \cdot \frac{1}{2} \cdot 2^N \cdot U_{\text{LSB}}. \quad (30)$$

The resulting  $\text{SNR}_{\text{ADC}}$  caused by the quantization error is

$$\text{SNR}_{\text{ADC}} = 20 \cdot \log \left[ \frac{U_{s,\text{RMS}}}{U_{e,\text{RMS}}} \right] = (1.8 + 6 \cdot N) \text{dB}. \quad (31)$$

High speed flash type ADCs with a conversion rate of several tens of megasamples per second usually are available with  $N = 8$ . So, the maximum SNR to achieve for the signal detection is limited by (31) to approximately 50 dB for a 100% modulation depth. With a 50% modulation, the achievable  $\text{SNR}_{\text{ADC}}$  is reduced to 44 dB. As shown in Section VI, this is sufficient for most applications and does not degrade the system's performance noticeably. Therefore, it is important to apply an automatic gain control (or a logarithmic amplifier) in the receiver.

Amplitude measurement is important for the quadrature detection. An error in amplitude digitization measurement causes an error in phase. For 8-bit quantization

and 100% modulation of signal, the phase error caused by quantization is about 0.5 degrees.

In addition to the quantization error, ADCs are afflicted with offset errors and nonlinearities, causing further errors. Usually, these errors are smaller than the quantization error, and, because they are reproducible, they can be coped with by a calibration process.

## VI. DISCUSSION

Until now in literature, sensitivity, accuracy, and resolution usually were given simultaneously with a maximum distance range for radio request. Errors caused by a SNR decreasing with distance and those caused by other error sources had been disregarded. Here, it is shown, by means of practical examples, that, for actual system designs, these errors have to be considered too. Some numerical examples with frequently used parameters are given.

In an application for temperature measurement, we employed a delay time radio sensor with a delay of  $5 \mu\text{s}$ , operating at 869 MHz. Coherent phase detection was performed for time measurement. Amplitude errors were less important for the application. They only would apply if time were evaluated by measurement of the time between threshold crossing. In our example, we look for a measurement resolution of  $> 10^{-5}$  achieved in  $> 99.9\%$  of radio interrogation cycles.

Utilizing a  $\text{LiNbO}_3$  SAW DL with a 92 ppm/K TK,  $10^{-5}$  resolution corresponds to a temperature resolution of approximately 10 mK. With  $T_{\text{period}} = 1/(869 \cdot 10^6) \text{ s} = 1.15 \text{ ns}$ ,  $2\pi$  corresponds to  $2.30 \cdot 10^{-4}$  of the  $5\text{-}\mu\text{s}$  delay. To achieve a resolution of  $10^{-5}$ , a phase uncertainty of 15 degrees is admissible as a maximum. For  $10^{-6}$ , a maximum phase error of approximately 1.5 degrees would be allowed. For estimation of the total error, the noise power of all statistically independent error sources have to be added. The effect of phase noise is neglected here, assuming high-Q SAW resonator referenced oscillators in the system.

For high resolution requirements, the adjustment of the receiver is critical. With standard adjustment of low cost systems, e.g., 10%  $Q/I$  unbalance  $b/a$  and a 5 degree phase misadjustment  $\eta$ , up to approximately 6 degree phase uncertainty occurs, caused by the system itself. Therefore, the maximum resolution without noise effects is approximately  $4 \cdot 10^{-6}$ , only to be exceeded by exact tuning of the system.

On the other hand, to achieve the  $10^{-5}$  resolution of our example, a margin of 9 degrees for the phase error can be used. From Fig. 14, the SNR, necessary to keep the error limit in 99.9% of interrogation cycles, is found to be  $> 21 \text{ dB}$ . Employing an exactly tuned system ( $\eta = 0^\circ$ ,  $b/a = 1$ ) for a precision measurement with a resolution of  $10^{-6}$  (e.g., 1 mK for temperature), the phase error must be  $< 1.5$  degrees. With a  $\text{SNR} > 40 \text{ dB}$ , this is provided in 99.0% of measurements.

The maximum distance range can be found from the link budget in Fig. 7. Assuming a gain of the antennas

$G_{\text{sens}}$  [dB] at the sensor and  $G_{\text{sys}}$  [dB] at the interrogation system, a transmitted power  $P_t$  [dBm], a sensor attenuation (the insertion loss of the SAW sensor)  $a_{\text{sensor}}$  [dB], and a coherent integration over  $N$  request cycles, the maximal path attenuation  $a_{\text{path}}$  [dB] is calculated from

$$a_{\text{path}} \leq P_t + 2 \cdot G_{\text{sys}} + 2 \cdot G_{\text{sens}} - a_{\text{sensor}} - \text{SNR} + 10 \cdot \log(N) - M - F_{\text{mm}} - N_0 - 10 \cdot \log(B/1 \text{ Hz}) - \text{NF}. \quad (32)$$

In (32),  $N_0 = k \cdot \vartheta$  [dBm/Hz] means the thermal noise on the radio channel, and  $F_{\text{mm}}$  [dB] is the additional noise figure caused by the collected man-made noise. The term NF [dB] is the noise figure of the receiver, and  $B$  [Hz] is its bandwidth.  $M$  [dB] represents a margin for fading caused by the radio propagation, etc.

From (32), the sum of SNR and total transmission loss  $a_{\text{path}}$  is calculated. For example, we assume  $P_t = 20$  dBm,  $G_{\text{sys}} = G_{\text{sens}} = 0$  dB,  $a_{\text{sens}} = 20$  dB,  $N_0 = -174$  dBm/Hz,  $B = 1.7$  MHz, NF = 10 dB,  $M = 10$  dB, and  $N = 1$ . Then, the sum of path loss (up- and downlink) and SNR is calculated to be a maximum of 90 dB. Therefore, with the approximate 20-dB SNR for a resolution better than  $10^{-5}$  in more than 99.99% of measurement cycles without coherent integration, a unidirectional path loss of approximately 35 dB is allowed. For a 433.92-MHz radio transmission with an exponent  $p = 2$  in (16), a distance of 3.1 can be bridged without obstacles and without destructive interference caused by multipath propagation. For the  $10^{-6}$  resolution with the well-tuned request system, about a 1-m range is feasible with the parameters mentioned previously. A doubled distance means a total bidirectional attenuation enhanced by 12 dB.

An enhancement of distance range is achieved by coherent integration for  $N$  measurement cycles. Theoretically, this is a linear process; actually the gain is limited by the dynamic range of the receiver and by phase stability of the LOs and movements. In our experiments, an integration of up to 256 measurements was performed without significant losses, yielding a gain of approximately 24 dB in energy.

For systems operated in an electromagnetically polluted environment, co-channel interference from ISM band communication systems cause an additional phase error. To keep this error  $< 1$  degree, an approximate 40-dB SIR (Fig. 15) is required.

Reducing the bandwidth because of a longer radio signal, e.g., for radio request of high- $Q$  resonators or passive nonlinear sensors, the distance range is enhanced because of the smaller noise power received caused by the narrower receiver bandwidth.

The SNR also is enhanced by methods enhancing the signal's energy, expanding the transmitted impulse to a signal with a long duration in time and wide bandwidth and applying impulse compression.

Employing a measurement of amplitude, e.g., for radio request of impedance loaded SAW transponders, a very similar calculation can be applied. The resolution for these sensor systems is approximately 1%, if amplitude

measurement is performed exclusively. Assuming the same parameters for frequency and adjustment of the request system ( $|(b-a)/a| \leq 10\%$ ,  $\eta \leq 5$  degree), the amplitude error from this poor tuning is up to 12%, degrading the overall performance heavily.

Again, employing a tuned system, from Fig. 13, the SNR required to achieve an amplitude error, with the parameter probability of exceeding a limit of  $w$  times the amplitude, is found. To provide an amplitude error  $< 5\%$  for at least 99% of the samples, a SNR of  $> 33$  dB is necessary. In comparison with the example mentioned previously, a much better quality of the received response signal is required to achieve sufficient performance. The maximum amplitude error caused by interference is equal to the square root of the SIR, e.g., 1% for 40 dB.

Employing frequency measurement, the relative frequency error  $\Delta f/f$  is calculated from the phase error  $\Delta\varphi$ . According to (20), the frequency measurement error of a decaying 433-MHz resonator's signal with a  $T_m = 5 \mu\text{s}$  and a phase error of 15 degrees (SNR  $\approx 21$  dB) is approximately 20 ppm, small in comparison with the SAW manufacturing tolerances.

## VII. APPLICATIONS

In recent years, a lot of applications have been presented. Here, only a brief overview with reference to the publications can be given. In the first applications, measurement of temperature with identification tags were performed. Lithiumniobate SAW devices have been mounted on disc brakes of railway cars to monitor the temperature experimentally [5]. Then, the SAW sensors were affected directly in many ways. As shown in [3] and [5]–[9] by bending, stretching, and compressing the SAW substrate, sensors for torque, force, displacement, vibration, acceleration, etc. were made. Sensors for the “intelligent tire” have been developed to monitor the tire pressure [5] as well as the friction between the tire and the road surface [29]. With the introduction of the indirectly affected impedance loaded SAW transponders [28], [30], a lot of further applications became feasible. Today, sensor circuits for humidity, pressure, position, acceleration, wear, magnetic field [31], and electric current are known; others are in development.

SAW sensors require a more extensive interrogation system than active and semi active radio sensors. They can compete in special applications, where the sensors have to withstand severe conditions because of heat, radiation, or electromagnetic fields and where the sensors are required to have a long life time free of maintenance.

## VIII. CONCLUSION

In the paper, the actual state of passive SAW sensor technology has been reviewed. A survey of the parameters was given, which is necessary for the design of an actual

sensor system. First, the sensors were described. Then, the methods of radio interrogation were investigated. A division into FDS and TDS was suggested. The methods of parameter detection, data reduction measures, energy enhancement, and multiple access techniques have been discussed. Multiple access to a number of sensors is difficult because of their passive properties. Space and time division are actually proven. The effects of radio transmission to the system design have been evaluated. An extensive part of the paper dealt with the uncertainty of the measurement, the occurring errors, and their origins. In a discussion, the parameters of actual employed sensor systems have been indicated. It was found that phase detection is much more robust against misadjustment of the receiver and noise errors. It is suggested to be used advantageously.

For high speed measurements, wideband delay line sensors are best combined with a burst radio request and TDS. For further data reduction, sample on demand signal processing is applied. So, a radio interrogation of passive sensors is feasible with high resolution for short range applications. It was found, that a low cost system with coherent phase detection is well suited for measurements with an uncertainty of  $< 10^{-5}$ , corresponding to approximately 10 mK for temperature measurements over a distance range of approximately 1 m. Similar to this, a high-Q SAWR can be interrogated with a sufficient accuracy.

To achieve a higher distance range of operation or a better precision, tuned systems including integration measures are required. This is done by utilizing spread spectrum signals, e.g., chirps, or by reducing the bandwidth, enlarging the signal's duration. Energy enhancement also is done by signal integration. A gain in energy, almost proportional to the sum of the integrated energy parts, is achieved by coherent integration. Noncoherent integration only is capable of working well above a threshold of signal quality. Applying SAW transponders, a high measurand bandwidth is achieved with external conventional sensors. The uncertainty is relatively high if amplitude detection is employed only.

Applying the proper radio request with suitable total response signal's energy and signal processing method, TDS and FDS yield the same performance of measurement for applications without stringent requirements for short measurement time.

Finally, some applications of SAW sensors were shown. Passive radio sensors have been presented first only a few years ago. Since then, the field of applications is rapidly growing. Today, the first industrial implementations are in development, initialized, and supported by our investigations. In a world of increasing demand for sensors, it is foreseeable that SAW sensors will replace conventional sensors, disclose new applications, and find a fixed position for more than special applications for which other technologies cannot be employed.

## ACKNOWLEDGMENT

The author thanks Prof. Franz Seifert for many discussions and scientific and practical advice. The author also gratefully acknowledges the support and stimulating discussions with Dr. L Reindl, Dr. C.C.W. Ruppel, and W.E. Bulst from Siemens ZT KM 1, Munich, Germany. Last but not least, thanks to all colleagues, especially, Dr. G. Ostermayer, R. Steindl, Ch. Hausleitner, M. Brandl, and all diploma students who accompanied these activities for several years.

## REFERENCES

- [1] A. Pohl, "New passive sensors," in *Proc. IEEE Instrum. Meas. Technol. Conf.*, Venice, Italy, pp. 1251–1255, 1999.
- [2] W. Buff, "SAW sensors," *Sens. Actuators*, vol. A42, pp. 117–121, 1992.
- [3] F. Seifert, W. E. Bulst, and C. Ruppel, "Mechanical sensors based on surface acoustic waves," *Sens. Actuators*, vol. A44, pp. 231–239, 1994.
- [4] E. Benes, M. Gröschl, F. Seifert, and A. Pohl, "Comparison between BAW and SAW sensor principles," *IEEE Trans. Ultrason., Ferroelect., Freq. Contr.*, vol. 45, no. 5, pp. 1314–1330, Sep. 1998.
- [5] A. Pohl and F. Seifert, "Wirelessly interrogable SAW sensors for vehicular applications," in *Proc. IEEE Instrum. Meas. Conf.*, Brussels, Belgium, pp. 1465–1468, 1996.
- [6] A. Pohl, "Measurements of vibration and acceleration utilizing SAW sensors," in *Proc. SENSOR 99*, Germany, vol. 2, pp. 53–58.
- [7] A. Pohl, G. Ostermayer, L. Reindl, and F. Seifert, "Monitoring the tire pressure at cars using passive SAW sensors," in *Proc. IEEE Ultrason. Symp.*, Toronto, pp. 471–474, 1997.
- [8] A. Pohl, A. Springer, L. Reindl, F. Seifert, and R. Weigel, "New applications of wirelessly interrogable passive SAW sensors," in *Proc. MTT-S*, Baltimore, MD, pp. 503–506, 1998.
- [9] A. Pohl and R. Steindl, "Measurement of mechanical parameters utilizing passive sensors," in *Proc. Mechatronics '98*, Sweden, pp. 571–576, 1998.
- [10] A. Pohl, R. Steindl, L. Reindl, and F. Seifert, "Wirelessly interrogable sensors for different purposes in industrial radio channel," in *Proc. IEEE Ultrason. Symp.*, Sendai, Japan, pp. 347–350, 1998.
- [11] P. A. Nysen, H. Skeie, and D. Armstrong, "System for interrogating a passive transponder carrying phase-encoded information," U.S. Patent 4725841; 4 625 207; 4 625 208, 1983–1986.
- [12] W. E. Bulst and C.C.W. Ruppel, "Akustische Oberflächenwellentechnologie für innovationen," *Siemens Rev.*, pp. 33–38, Spring 1994.
- [13] Ch. E. Cook and M. Bernfeld, *Radar Signals*. Norwood, MA: Artech House, 1993.
- [14] F. Seifert, A. Pohl, G. Ostermayer, and G. Berger, "Wireless sensors and data links based on SAW devices," presented at IEEE MTT/AP and UFFC Chapter Workshop, Sindelfingen, Germany 1997.
- [15] L. Reindl and W. Ruile, "Programmable reflectors for SAW-ID-Tags," *Proc. IEEE Ultrason. Symp.*, Baltimore, MD, pp. 125–130, 1993.
- [16] A. Pohl, C. Posch, L. Reindl, and F. Seifert, "Digitally controlled compressive receiver," in *Proc. IEEE Int. Symp. Spread Spectrum Techniques Appl.*, Mainz, Germany, pp. 409–413, 1996.
- [17] A. Pohl, G. Ostermayer, and F. Seifert, "Wireless sensing using oscillator circuits locked to remote high-Q SAW resonators," in *IEEE Trans. Ultrason., Ferroelect., Freq. Contr.*, vol. 45, no. 5, pp. 1161–1168, Sep. 1998.
- [18] A. Pohl, "A low cost high definition wireless sensor system utilizing intersymbol interference," *IEEE Trans. Ultrason., Ferroelect., Freq. Contr.*, vol. 45, no. 5, pp. 1355–1362, Sep. 1998.
- [19] G. Ostermayer, A. Pohl, L. Reindl, and F. Seifert, "Multiple access to SAW sensors using matched filter properties," in *Proc. IEEE Ultrason. Symp.*, Toronto, Canada, pp. 339–342, 1997.

- [20] G. Ostermayer, A. Pohl, C. Hausleitner, L. Reindl, and F. Seifert, "CDMA for wireless SAW sensor applications," in *Proc. IEEE Int. Symp. Spread Spectrum Techniques Appl.*, pp. 795–799, 1996.
- [21] G. Ostermayer, A. Pohl, R. Steindl, and F. Seifert, "SAW sensors and correlative signal processing - A method providing multiple access capability," in *Proc. ISSSTA 98*, South Africa, pp. 902–906.
- [22] T. S. Rappaport, *Wireless Communications — Principles & Practice*. Piscataway, NJ: IEEE Press, pp. 139–196.
- [23] Siemens Matsushita, databook, SAW components, 1996.
- [24] A. Pohl and F. Seifert, "New applications of wirelessly interrogable passive SAW sensors," in *IEEE Trans. Microwave Theory Tech.*, vol. 46, Part II, no. 12, pp. 2208–2212, Dec. 1998.
- [25] J. K. Holmes, *Coherent Spread Spectrum Systems*. Malabar, FL: Krieger Publishing Co., 1990.
- [26] J. G. Proakis and M. Salehi, *Communication Systems Engineering*. Prentice Hall International, 1994.
- [27] A. Pohl and R. Steindl, "A new generation of passive radio requestable SAW sensors for ultrafast measurements," in *Proc. IEEE Instrum. Meas. Conf.*, Venice, Italy, pp. 1728–1733, 1999.
- [28] A. Pohl, "The intelligent tire — Measurement of tire friction with passive SAW sensors," unpublished.
- [29] R. Steindl, A. Pohl, and F. Seifert, "Impedance loaded SAW sensors offer a wide range of measurement opportunities," in *Proc. IEEE MTT-S 1999*, Anaheim, CA, pp. 1453–1456.
- [30] R. Steindl, Ch. Hausleitner, A. Pohl, H. Hauser, and J. Nicolics, "Giant magneto-impedance magnetic field sensor with surface acoustic wave technology," in *Proc. Eurosensors 1999*, Delft, The Netherlands,



**Alfred Pohl** (M'95) was born in Austria in 1963. He received the Dipl.-Ing. and the Dr. degree from the University of Technology in Vienna. There, he currently works as an assistant professor, teaching circuit design and topics related to communication engineering.

His research interests are in the fields of spread spectrum communication and surface acoustic wave devices. Current activities are focused on passive SAW sensors, advanced radio request principles, and new applications.